

# **SOL and Divertor physics**

---

Nicola Vianello

28 November 2024

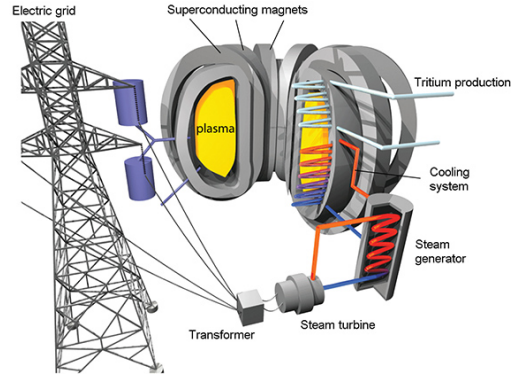
ISTP-CNR and Consorzio RFX

# **Introduction**

---

# The motivation for a divertor: the exhaust problem

- Nuclear reaction

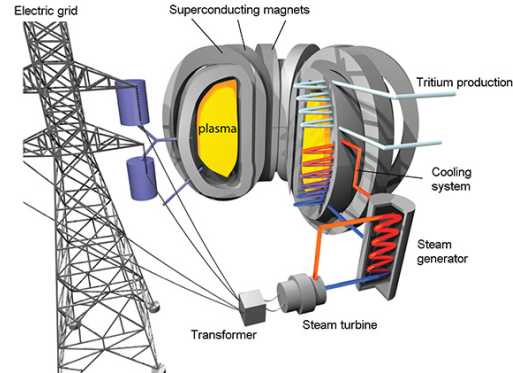


# The motivation for a divertor: the exhaust problem

- Nuclear reaction



- Neutrons leave the plasma into power conversion system and will be used for net energy production

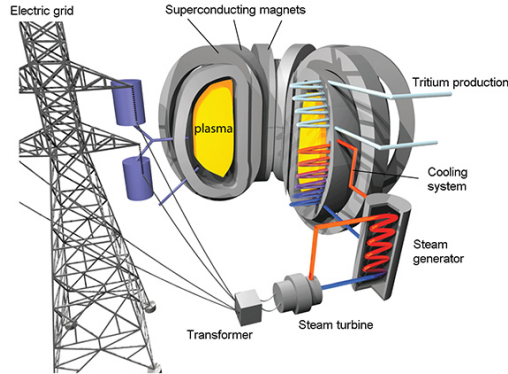


# The motivation for a divertor: the exhaust problem

- Nuclear reaction



- Neutrons leave the plasma into power conversion system and will be used for net energy production
- Alphas heat the plasmas and then need to be exhausted



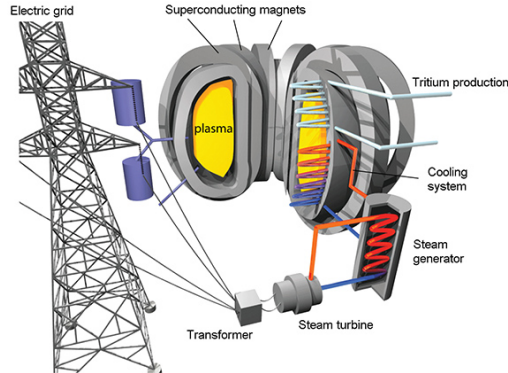
# The motivation for a divertor: the exhaust problem

- Nuclear reaction



- Neutrons leave the plasma into power conversion system and will be used for net energy production
- Alphas heat the plasmas and then need to be exhausted
- The roles:

- Helium ash removal
- Impurity control
- Fueling Neutral particle control
- Heat Exhaust
- Minimize material damage as erosion and melting



## Severity of the exhaust problem



### ASDEX-Upgrade

Major radius: 1.65m

$$q_{\perp} \approx 40 \text{ MW/m}^2$$

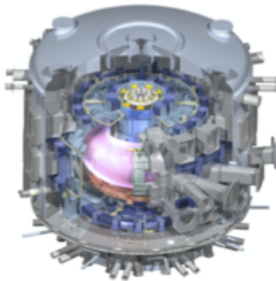
## Severity of the exhaust problem



**ASDEX-Upgrade**

Major radius: 1.65m

$q_{\perp}$  40 MW/m<sup>2</sup>



**ITER**

Major radius: 6.2m

$q_{\perp}$  100 MW/m<sup>2</sup>

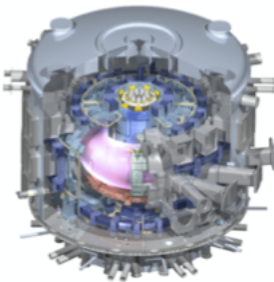
## Severity of the exhaust problem



**ASDEX-Upgrade**

Major radius: 1.65m

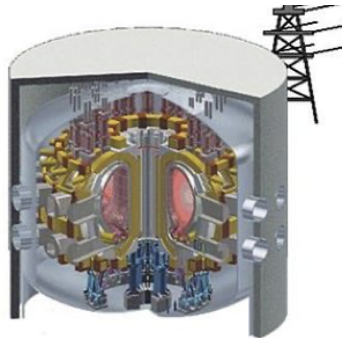
$q_{\perp}$  40 MW/m<sup>2</sup>



**ITER**

Major radius: 6.2m

$q_{\perp}$  100 MW/m<sup>2</sup>

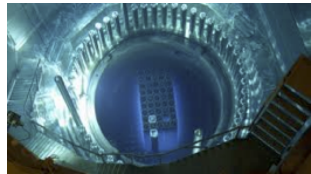


**DEMO**

Major radius: ~ 9m

$q_{\perp}$  350 MW/m<sup>2</sup>

## Severity of the exhaust problem



$$q_{\perp} \sim 1 \text{MW}^2$$



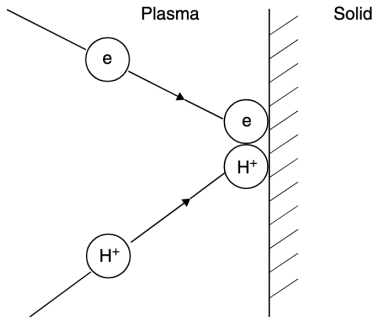
$$q_{\perp} \sim 5 \text{MW}^2$$



$$q_{\perp} \sim 80 \text{MW}^2$$

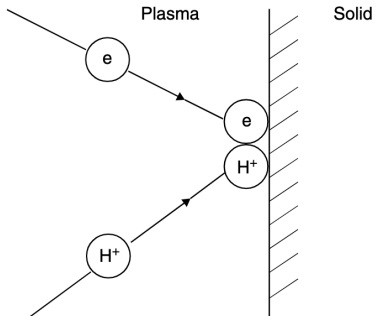
## Solid surface interaction with a plasma: PWI

- Any solid surface inserted into a plasma constitutes a very strong particle sink
- If charged particles strike a solid surface they tend to stick long enough to recombine
- For insulating or electrically isolated surfaces, opposite charges stick and produce *surface recombination*
- The neutrals are generally weakly bound to the solid and are thermally re-emitted as neutrals



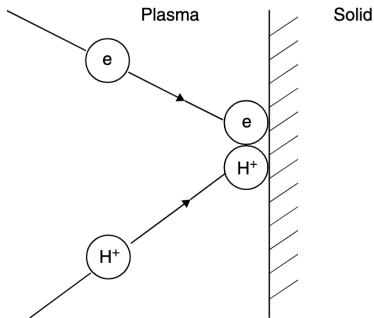
## Solid surface interaction with a plasma: PWI

- Any solid surface inserted into a plasma constitutes a very strong particle sink
- If charged particles strike a solid surface they tend to stick long enough to recombine
- For insulating or electrically isolated surfaces, opposite charges stick and produce *surface recombination*
- Thus we have a plasma sink not a mass sink



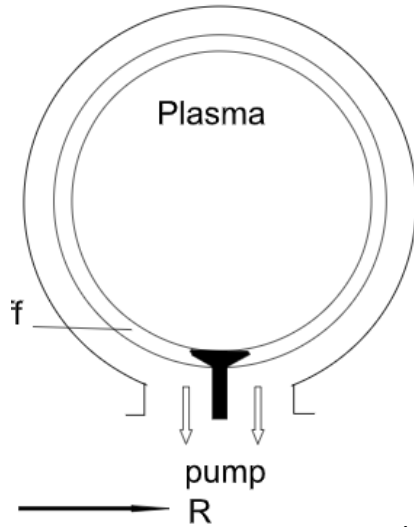
## Solid surface interaction with a plasma: PWI

- Any solid surface inserted into a plasma constitutes a very strong particle sink
- If charged particles strike a solid surface they tend to stick long enough to recombine
- For insulating or electrically isolated surfaces, opposite charges stick and produce *surface recombination*
- Thus we have a plasma sink not a mass sink
- This *recycling* process can happen in steady-state condition whereby plasma charged pairs are lost at the same rate as recombined neutrals re-enter the plasma



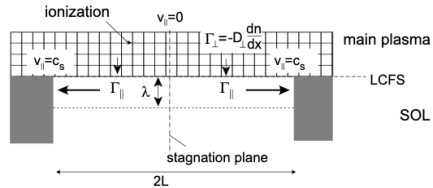
## The Limiter configuration and simple SOL

- Solid surface eventually inserted by purpose to provide controlled Plasma Wall Interaction
- Historically first solution proposed is the **limiter solution** (with toroidal or poloidal limiters)
- Clear identification of the **LCFS** and the SOL
- Can be described by **fluid approach** as far as **self collisional mean free paths of electrons and ions lower than parallel connection length  $\lambda_{ee}, \lambda_{ii} \ll L_{||}$**



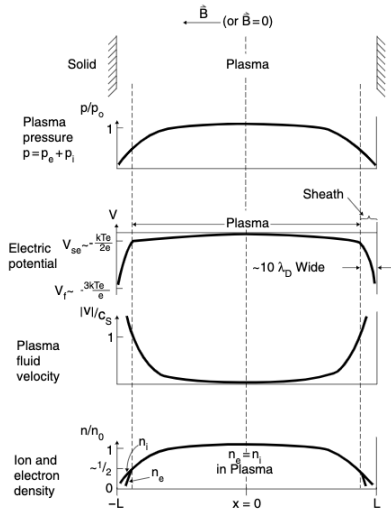
## The Limiter configuration and simple SOL

- If the neutral m.f.p. is long enough to pass through the SOL and they are ionized inside the main plasm, then we are in the condition of **Simple SOL**
- To describe the characteristics of simple SOL we need to describe better the interaction of a plasma with solid wall



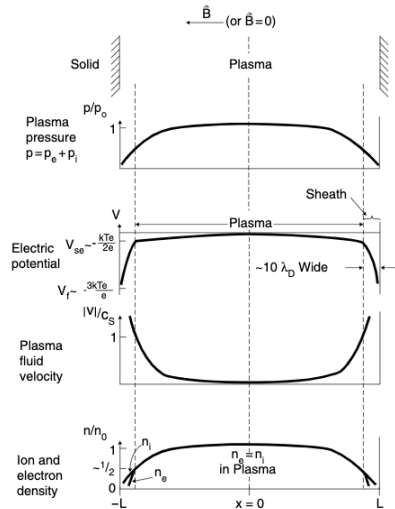
# The Limiter configuration and simple SOL

- In presence of a solid wall higher electron mobility charge up the wall negatively  $\Rightarrow$  ambipolar electric field builds up to ensure equal ion/electron loss  $\rightarrow V_{wall} \approx -3kT_e/e$  w.r.t. plasma potential



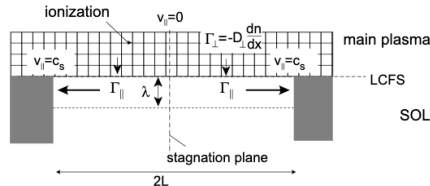
# The Limiter configuration and simple SOL

- In presence of a solid wall higher electron mobility charge up the wall negatively  $\Rightarrow$  ambipolar electric field builds up to ensure equal ion/electron loss  $\rightarrow V_{wall} \approx -3kT_e/e$  w.r.t. plasma potential
- Electrostatic potential shielded within a Debye length  $\lambda_D = \sqrt{\frac{\epsilon_0 k T_e}{n_e e^2}}$
- Shielding is not perfect. pre-sheath electric field of the order of  $E \approx kT_e/2eL$
- Ions are accelerated in the pre-sheath up to the sheath entrance velocity  $v_{se} = c_s = \sqrt{\frac{k(T_e + T_i)}{m_i}} \Rightarrow$  Bohm criterion
- At sheath entrance density is  $n_{se} = \frac{1}{2} n_0$



# The Limiter configuration and simple SOL

- In the **simple SOL approximation** with no source of particle in the SOL, simple relation holds between **diffusion** and **SOL width**
- This is obtained by the equality between the **Total particle outflow crossing the LCFS**  $\phi_{\perp}$  to the **total particle flow towards the 2 solid surfaces**  $\phi_{\parallel}$

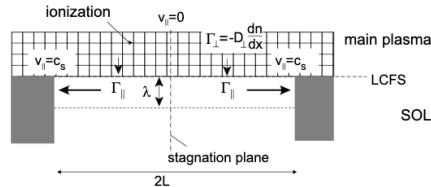


$$\phi_{\perp} = -D_{\perp}^{SOL} \frac{dn}{dr}_{LCFS} 2Lw = -D_{\perp}^{SOL} \frac{n_{LCFS}}{\lambda_n} 2Lw$$

$$\phi_{\parallel} = 2w \int_{r=LCFS}^{\infty} n c_s dr \approx 2w \frac{1}{2} n_{LCFS} c_s \lambda_n \quad \text{with} \quad n(r) = n_{LCFS} e^{-\frac{r}{\lambda_n}}$$

# The Limiter configuration and simple SOL

- In the **simple SOL approximation** with no source of particle in the SOL, simple relation holds between **diffusion** and **SOL width**
- This is obtained by the equality between the **Total particle outflow crossing the LCFS**  $\phi_{\perp}$  to the **total particle flow towards the 2 solid surfaces**  $\phi_{\parallel}$



$$\lambda_n = \sqrt{\frac{2D_{\perp}^{SOL} L}{c_s}}$$

## The Limiter configuration and simple SOL

- The corresponding ion and electron parallel flux to the target can be estimated remembering that electrons distributions remains Maxwellian even in retarding electric field

$$\Gamma_t^i = n_{se} c_s, \quad \Gamma_t^e = \frac{1}{4} n_{es} \exp(eV_s/kT_e) \sqrt{\frac{8kT_e}{\pi m_e}} \quad \Rightarrow \frac{eV_s}{kT_e} = 0.5 \ln \left( 2\pi \frac{m_e}{m_i} \right) (1 + T_i/T_e) \approx 3$$

## The Limiter configuration and simple SOL

- The corresponding ion and electron parallel flux to the target can be estimated remembering that electrons distributions remains Maxwellian even in retarding electric field

$$\Gamma_t^i = n_{se} c_s, \quad \Gamma_t^e = \frac{1}{4} n_{es} \exp(eV_s/kT_e) \sqrt{\frac{8kT_e}{\pi m_e}} \quad \Rightarrow \frac{eV_s}{kT_e} = 0.5 \ln \left( 2\pi \frac{m_e}{m_i} \right) (1 + T_i/T_e) \approx 3$$

- Heat flux related to particle flux through the **sheath transmission coefficients**  $\gamma_{i,e} = \frac{q_{i,e}}{kT_e \Gamma_t}$

## The Limiter configuration and simple SOL

- The corresponding ion and electron parallel flux to the target can be estimated remembering that electrons distributions remains Maxwellian even in retarding electric field

$$\Gamma_t^i = n_{se} c_s, \quad \Gamma_t^e = \frac{1}{4} n_{es} \exp(eV_s/kT_e) \sqrt{\frac{8kT_e}{\pi m_e}} \quad \Rightarrow \frac{eV_s}{kT_e} = 0.5 \ln \left( 2\pi \frac{m_e}{m_i} \right) (1 + T_i/T_e) \approx 3$$

- Heat flux related to particle flux through the **sheath transmission coefficients**  $\gamma_{i,e} = \frac{q_{i,e}}{kT_e \Gamma_t}$
- For electrons considering sheath and pre-sheath drop  $\gamma_e = 5.5$
- For the ion the computation is not straightforward: if ion distribution is maxwellian then  $\gamma_i = 3.5$

## The Limiter configuration and simple SOL

- The corresponding ion and electron parallel flux to the target can be estimated remembering that electrons distributions remains Maxwellian even in retarding electric field

$$\Gamma_t^i = n_{se} c_s, \quad \Gamma_t^e = \frac{1}{4} n_{es} \exp(eV_s/kT_e) \sqrt{\frac{8kT_e}{\pi m_e}} \quad \Rightarrow \frac{eV_s}{kT_e} = 0.5 \ln \left( 2\pi \frac{m_e}{m_i} \right) (1 + T_i/T_e) \approx 3$$

- Heat flux related to particle flux through the **sheath transmission coefficients**  $\gamma_{i,e} = \frac{q_{i,e}}{kT_e \Gamma_t}$
- For electrons considering sheath and pre-sheath drop  $\gamma_e = 5.5$
- For the ion the computation is not straightforward: if ion distribution is maxwellian then  $\gamma_i = 3.5$
- The flux is then computed as  $q_t^{i,e} = \gamma_{i,e} n_{es} c_s kT_e$

## General description of the parallel transport in the SOL

- Identified the ion and electron heat flux to the target as related to the corresponding particle flux
- Need to determine the eventual spatial distribution. 1D approach with detail description in (P. C. Stangeby 2000; Unterberg 2017)

## General description of the parallel transport in the SOL

- Density conservation equation in steady-state

$$\frac{\partial}{\partial z} (n_{i,e} V_{\parallel i,e}) = S_p$$

- Ion momentum conservation in steady state

$$\frac{\partial}{\partial z} (m_i n v_{\parallel i}^2 + p_i) = e n E + R_{ie} + R_n$$

- $R_{ie}$  being the friction force caused by electron collisions:

$$R_{ie} = m_e (v_e - v_i) \nu_{ei} n + 0.71 n \partial k T_e / \partial z$$

- $R_n$  being the friction force due to collisions with neutrals

$$R_n = -m_i (v_i - v_n) \langle \sigma v \rangle_{CX} n_n n + m_i v_n S_p \text{ where we implicitly assumed that momentum loss due to Charce eXchange is dominant mechanism for ions}$$

## General description of the parallel transport in the SOL

- Density conservation equation in steady-state

$$\frac{\partial}{\partial z} (n_{i,e} V_{\parallel i,e}) = S_p$$

- For the electron we rely on the small inertia and momentum balance is written as

$$\frac{\partial p_e}{\partial z} + enE = -m_e(v_e - v_i)\nu_{ei} - 0.71n \frac{\partial kT_e}{\partial z}$$

where we kept the friction term for ion-electron momentum exchange

## General description of the parallel transport in the SOL

- Density conservation equation in steady-state

$$\frac{\partial}{\partial z} (n_{i,e} V_{\parallel i,e}) = S_p$$

- The total plasma momentum equation results then in

$$\frac{\partial}{\partial z} (m_i n v^2 + p_i + p_e) = -m_i (v_i - v_n) \langle \sigma v \rangle n_n n + m_i v_n S_p(z)$$

- We recognize that the main force acting on  $m_i n v^2$  is the pressure gradient with no effect from electric field. Strong uncertainty come from the unknown of  $T_{\parallel}$
- We need to move to higher momentum and compute the parallel energy equation

## General description of the parallel transport in the SOL

- Ion energy conservation

$$\frac{\partial q_{\parallel,i}}{\partial z} = \frac{\partial}{\partial z} \left[ \left( \frac{5}{2} T_i + \frac{1}{2} m_i v_i^2 \right) n v_i \begin{bmatrix} -\kappa_{0,i} T_i^{5/2} \frac{\partial T_i}{\partial z} \end{bmatrix} \right] = e n v_i E + Q_{eq} + Q_{Ei}$$

- Electron energy conservation equation

$$\frac{\partial q_{\parallel,e}}{\partial z} = \frac{\partial}{\partial z} \left[ \frac{5}{2} T_e n v_e \begin{bmatrix} -\kappa_{0,e} T_e^{5/2} \frac{\partial T_e}{\partial z} \end{bmatrix} \right] = -e n v_i E - Q_{eq} + Q_r + Q_{Ee}$$

- With  $Q_{eq}$  arising because of thermal equilibration collision between electrons and ions,  $Q_r$  the Joule heating term,  $Q_{Ei}$  resulting from ion-neutral interaction and  $Q_{Ee}$  is the energy loss for electrons because of inelastic collisions which ionize or excite neutrals
- Ion conduction  $\kappa_{0,i} \approx 60 \ll \kappa_{0,e} \approx 2000$  because of a  $m^{-1/2}$  dependence

## General description of the parallel transport in the SOL

- For  $T_e = T_i$ , defining the total pressure  $p = p_e + p_i$  we have a simplified form

$$\frac{\partial(nv)}{\partial z} = S_p$$

$$\frac{\partial}{\partial z}[(m_i v^2 + 2kT)n] = -m_i v \langle \sigma v \rangle n n_n$$

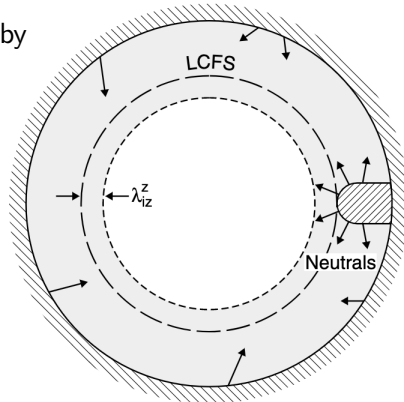
$$\frac{\partial}{\partial z} \left[ \left( \frac{1}{2} m_i v^2 + 5kT \right) nv - \kappa_{0,e} T_e^{5/2} \partial T_e / \partial z \right] = Q_r + Q_E$$

## **Divertor configuration**

---

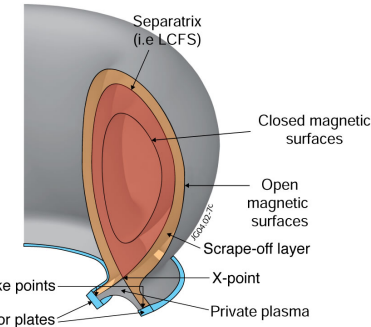
## Divertor configuration

- Limiter configuration not ideal to reduce plasma pollution by impurities generated by PWI



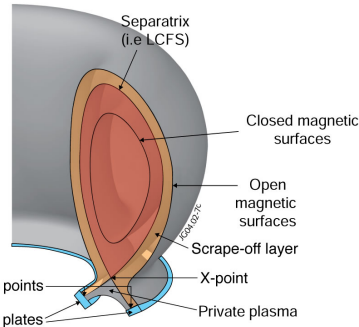
# Divertor configuration

- Limiter configuration not ideal to reduce plasma pollution by impurities generated by PWI
- Introduced the divertor configuration, generated by poloidal field coil where PWI occur far from confined region →  
**Ionization source in within SOL volume**
- Guarantee better pumping efficiency, lower heat flux at the target.



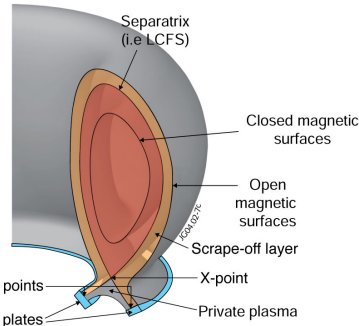
# Divertor configuration

- Limiter configuration not ideal to reduce plasma pollution by impurities generated by PWI
- Introduced the divertor configuration, generated by poloidal field coil where PWI occur far from confined region →  
**Ionization source in within SOL volume**
- Guarantee better pumping efficiency, lower heat flux at the target.
- Realized by reducing plasma temperature in front of the PFC and establishing a temperature gradient along the magnetic field



# Divertor configuration

- Limiter configuration not ideal to reduce plasma pollution by impurities generated by PWI
- Introduced the divertor configuration, generated by poloidal field coil where PWI occur far from confined region →  
**Ionization source in within SOL volume**
- Guarantee better pumping efficiency, lower heat flux at the target.
- Realized by reducing plasma temperature in front of the PFC and establishing a temperature gradient along the magnetic field
- Described by the **2 point model** (P. C. Stangeby 2018, 2000; P. Stangeby 2020a,b) which describe relation between upstream and target condition



## Divertor configuration

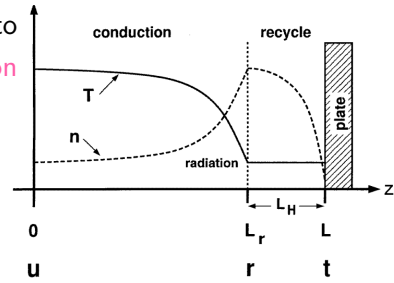
- Unfolding the SOL, if ionization occurs in a region close to the target, the **heat conduction** dominates  $\Rightarrow$  **conduction limited regime**
- The parallel heat flux is thus related to the parallel temperature gradient:

$$q_{\parallel} = \frac{P_{SOL}}{A_{\parallel}} = -\kappa_{0,e} T^{5/2} \frac{\partial T}{\partial z_{\parallel}}$$

- Integrating the previous equation

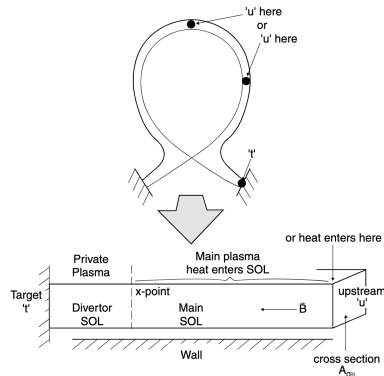
$$T(z_{\parallel}) = \left[ T_t^{7/2} + \frac{7}{2} \frac{P_{SOL}/A_{\parallel}(L_{\parallel} - s_{\parallel})}{\kappa_{0,e}} \right]$$

which for  $T_u \ll T_t$  we obtain  $T_u \simeq \left( \frac{7}{2} \frac{P_{SOL}/A_{\parallel} L_{\parallel}}{\kappa_{0,e}} \right)^{2/7}$



## Unfolding the SOL: 2 point model

- **Particle balance:** neutrals recycling from the targets are ionized in thin layer close to the target and parallel flow limited to the same region where particle accelerate up to sheath velocity entrance
- **Total pressure balance:**  $p + nmv^2 = \text{constant}$  which in the case of  $T_e = T_i$  implies  $p = 2nkT$  and dynamic pressure  $\neq 0$  only close to the target with  $v_t = c_{st} = \sqrt{2kT_t/m_i}$
- **Power balance:** Since  $v = 0$  almost entirely in the SOL then conduction dominated dynamic with  $T_u^{7/2} = T_t^{7/2} + \frac{7}{2}q_{\parallel}\frac{L_{\parallel}}{\kappa_{0e}}$ . No volumetric power loss assumed (very thin ionization layer) then  $q_{\parallel} = q_t = \gamma n_t k T_t c_{st}$



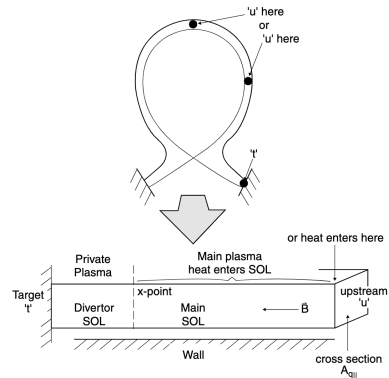
## Unfolding the SOL: 2 point model

- Combining all these information together we have:

$$2n_t T_t = n_u T_u$$

$$T_u^{7/2} = T_t^{7/2} + \frac{7}{2} q_{\parallel} \frac{L_{\parallel}}{\kappa_{0e}}$$

$$q_{\parallel} = q_t = \gamma n_t k T_t c_{st}$$



## Unfolding the SOL: 2 point model

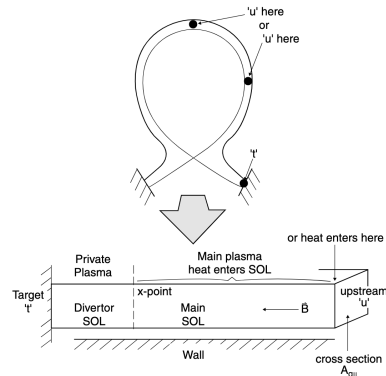
- We derive now  $n_t$ ,  $T_t$ ,  $T_u$  from  $n_u$  and  $q_{\parallel}$

$$T_u \simeq \left( \frac{7 q_{\parallel} L_{\parallel}}{2 \kappa_{0e}} \right)^{2/7}$$

$$T_t = \frac{m_i}{2e} \frac{4q_{\parallel}^2}{\gamma^2 e^2 n_u^2 T_u^2} \simeq \frac{m_i}{2e} \frac{4q_{\parallel}^2 \left( \frac{7 q_{\parallel} L_{\parallel}}{2 \kappa_{0e}} \right)^{-4/7}}{\gamma^2 e^2 n_u^2} \propto \frac{q_{\parallel}^{10/7}}{L_{\parallel}^{4/7} n_u^2}$$

$$n_t = \frac{n_u^3}{q_{\parallel}^2} \left( \frac{7 q_{\parallel} L_{\parallel}}{2 \kappa_{0e}} \right)^{6/7} \frac{\gamma^2 e^3}{4m_i} \propto [n_u^3] q_{\parallel}^{-8/7} L_{\parallel}^{6/7}$$

$$\Gamma_t = \frac{q_{\parallel}}{\gamma e T_T} = \frac{n_u^2}{q_{\parallel}} \left( \frac{7 q_{\parallel} L_{\parallel}}{2 \kappa_{0e}} \right)^{4/7} \frac{\gamma e^2}{2m_i} \propto n_u^2 q_{\parallel}^{-3/7} L_{\parallel}^{4/7}$$



## Modified 2Point Model

- We need to account the effect of **Volumetric power losses due to radiation and charge exchange losses**,  $q_{rad}^{SOL} + q_{CX}^{SOL} = f_{pow} q_{||}$  which modify the power balance equation as

$$(1 - f_{pow}) q_{||} = q_t = \gamma k T_t n_t c_{st}$$

- The momentum equation is modified to account for **momentum losses** which are due to volumetric momentum losses (e.g. friction with neutrals, viscous forces, volume recombination ) as well as *effective volumetric losses* due for example by cross-field transport:

$$2n_t T_t = f_{mom} n_u T_u$$

- Some residual convection still remain, which tend to reduce the temperature gradient. We therefore introduce a conduction factor  $f_{cond}$  so that  $q_{||,cond} = f_{cond} q_{||}$

## Modified 2Point Model

- The upstream temperature is modified accordingly and in the condition of  $T_t \ll T_u$  we have

$$T_u \simeq \left( \frac{2}{7} \frac{f_{cond} q_{||} L_{||}}{\kappa_0 e} \right)^{2/7} \propto f_{cond}^{2/7}$$

$T_u$  unaffected by momentum loss or volumetric power loss and small variation due to the convection

## Modified 2Point Model

- The upstream temperature is modified accordingly and in the condition of  $T_t \ll T_u$  we have

$$T_u \simeq \left( \frac{2}{7} \frac{f_{cond} q_{\parallel} L_{\parallel}}{\kappa_0 e} \right)^{2/7} \propto f_{cond}^{2/7}$$

$T_u$  unaffected by momentum loss or volumetric power loss and small variation due to the convection

- Target temperature strongly reduced by **volumetric power loss** and increase by **momentum loss**

$$T_t \propto \frac{(1 - f_{pow})^2}{f_{mom}^2 f_{cond}^{4/7}}$$

## Modified 2Point Model

- Correspondingly the ratio of upstream and target temperature results in

$$\frac{T_u}{T_t} \propto \frac{f_{cond}^{6/7} f_{mom}^2}{(1 - f_{pow}^2)}$$

with the clear tendency of convection to reduce/eliminate the parallel temperature gradient

- The target density results in

$$n_t \propto \frac{f_{mom}^3 f_{cond}^{6/7}}{(1 - f_{pow})^2}$$

We recognize a robust effect of momentum dissipation in suppressing target density

## Modified 2Point Model

- Finally the target particle flux is modified as

$$\Gamma_t \propto \frac{f_{mom}^2 f_{cond}^{4/7}}{1 - f_{pow}}$$

and thus with a strong contribution of **momentum loss** in reducing fluxes to the target

## Divertor regimes

For a given  $q_{\parallel u}$  input in a flux tube it is generally observed that as  $n_u$  is increased the target  $T_t$  decreases and the corresponding flux tube passes through **different regimes**:

1. **Sheath limited Regimes** where small temperature gradients exists and  $q_{\parallel}$  is constrained by sheath condition.  $\Gamma_{\parallel}$  and pressure approximately constant along the flux tube

## Divertor regimes

For a given  $q_{\parallel,u}$  input in a flux tube it is generally observed that as  $n_u$  is increased the target  $T_t$  decreases and the corresponding flux tube passes through **different regimes**:

1. **Sheath limited Regimes** where small temperature gradients exists and  $q_{\parallel}$  is constrained by sheath condition.  $\Gamma_{\parallel}$  and pressure approximately constant along the flux tube
2. **High Recycling Regime** a.k.a. *Conduction limited regime* where  $q_{\parallel}$  is constrained by sheath condition and temperature conduction. Significant drop of  $T_e$ ,  $T_t \ll T_u$ ,  $\Gamma_{\parallel,u} \ll \Gamma_{\parallel,t}$  but momentum is still constant along the flux tube

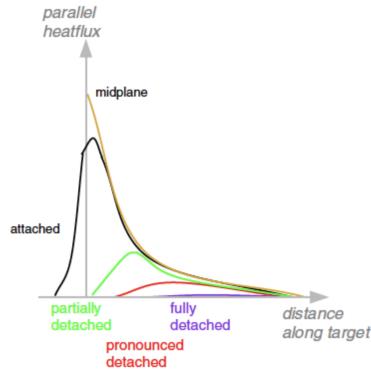
## Divertor regimes

For a given  $q_{\parallel u}$  input in a flux tube it is generally observed that as  $n_u$  is increased the target  $T_t$  decreases and the corresponding flux tube passes through **different regimes**:

1. **Sheath limited Regimes** where small temperature gradients exists and  $q_{\parallel}$  is constrained by sheath condition.  $\Gamma_{\parallel}$  and pressure approximately constant along the flux tube
2. **High Recycling Regime** a.k.a. *Conduction limited regime* where  $q_{\parallel}$  is constrained by sheath condition and temperature conduction. Significant drop of  $T_e$ ,  $T_t \ll T_u$ ,  $\Gamma_{\parallel,u} \ll \Gamma_{\parallel,t}$  but momentum is still constant along the flux tube
3. **Detachment regime** with significant reduction of the power and particle fluxes to the target with associated pronounced pressure drop

## Divertor regimes

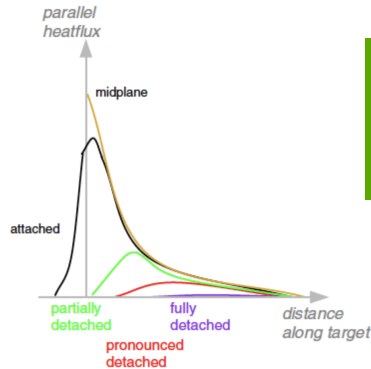
For a given  $q_{\parallel u}$  input in a flux tube it is generally observed that as  $n_u$  is increased the target  $T_t$  decreases and the corresponding flux tube passes through different regimes:



(Kallenbach *et al.* 2015)

## Divertor regimes

For a given  $q_{\parallel u}$  input in a flux tube it is generally observed that as  $n_u$  is increased the target  $T_t$  decreases and the corresponding flux tube passes through different regimes:

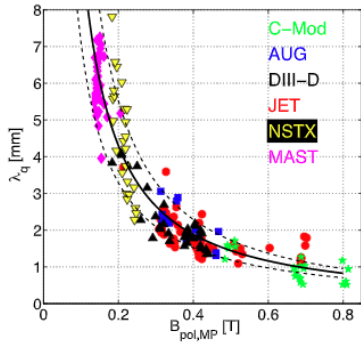


But what we can expect to be the  $\lambda_q$  in future devices?

## The need for exhaust solution: $\lambda_q$ scaling

- ITPA multi-machine database suggest **only the poloidal magnetic field is statistically important** (Eich *et al.* 2013)

$$\lambda_q = (0.63 \pm 0.08) B_{pol}^{-1.19 \pm 0.08}$$

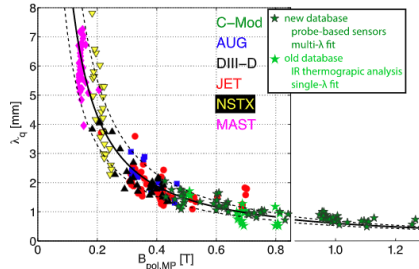


## The need for exhaust solution: $\lambda_q$ scaling

- ITPA multi-machine database suggest only the poloidal magnetic field is statistically important (Eich *et al.* 2013)

$$\lambda_q = (0.63 \pm 0.08) B_{pol}^{-1.19 \pm 0.08}$$

- Recent extension to ITER relevant poloidal magnetic field (Brunner *et al.* 2018) suggest the validity up to a predicted  $\lambda_q^{ITER} \leq 1\text{mm}$

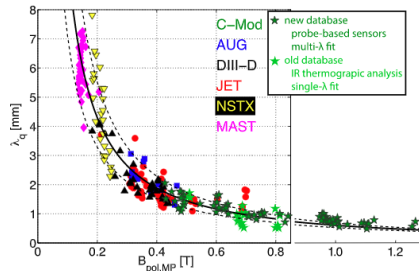


## The need for exhaust solution: $\lambda_q$ scaling

- ITPA multi-machine database suggest only the poloidal magnetic field is statistically important (Eich *et al.* 2013)

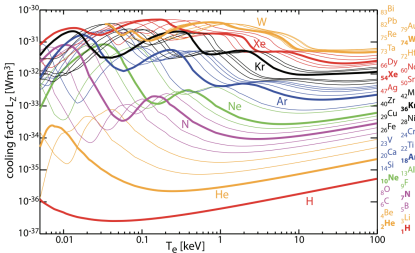
$$\lambda_q = (0.63 \pm 0.08) B_{pol}^{-1.19 \pm 0.08}$$

- Recent extension to ITER relevant poloidal magnetic field (Brunner *et al.* 2018) suggest the validity up to a predicted  $\lambda_q^{ITER} \leq 1\text{mm}$
- The predicted heat flux exceed the engineering material limit set to approximately  $10 \text{ M/m}^2$  or bit higher (to avoid W material re-crystallization (Pitts *et al.* 2019) ).  
We need mitigation strategy



# Radiative divertor

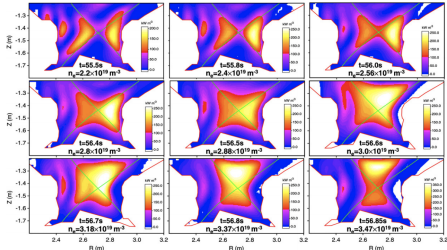
- Extrinsic impurity injected to increase radiation and provide tolerable heat load
- Scenario foreseen for ITER operation (Ne injection) to achieve partial detachment of the OSP
- For DEMO higher radiation fraction needed (90 % of  $P_{sep}$ ) needed



(Pütterich *et al.* 2019)

# Radiative divertor

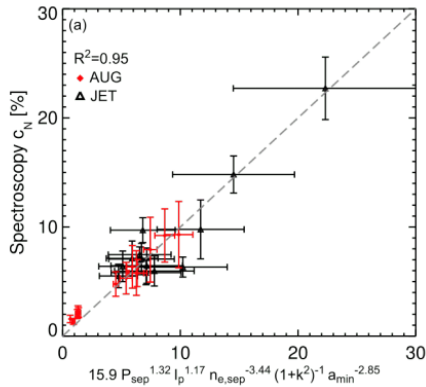
- Extrinsic impurity injected to increase radiation and provide tolerable heat load
- Scenario foreseen for ITER operation (Ne injection) to achieve partial detachment of the OSP
- For DEMO higher radiation fraction needed (90 % of  $P_{sep}$ ) needed
- Drawback appearance of a MARFE (multifaceted asymmetric radiation from the edge) and corresponding radiative collapse



(Huber *et al.* 2007)

## Radiative divertor

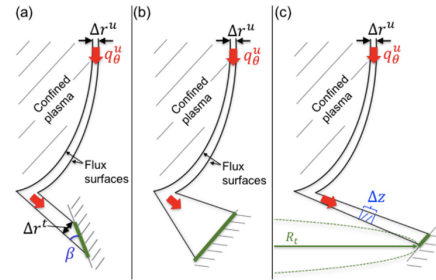
- Different models proposed for determining impurity concentration needed to provide detachment
  - **Goldston scaling** which focus on separatrix density (Goldston *et al.* 2017)  $c_z \propto \frac{P_{sep}}{B_p(1+\kappa)^{1.5} f_{GW,sep}^2}$
  - **Reinke scaling** which focus on machine size (Reinke 2017)  $c_z \propto B_T^{0.88} R^{1.33}$
  - **Kallenbach scaling** which focus on momentum and energy loss  $c_z \propto \frac{P_{sep}/R}{p_{div} \lambda_{int} R^{rz}}$
- Experimental results on multimachine scaling provide hints towards Goldstone scaling with a further dependence on minor radius



(Henderson, IAEA 2020, IAEA2023)

# Geometrical effects on heat flux

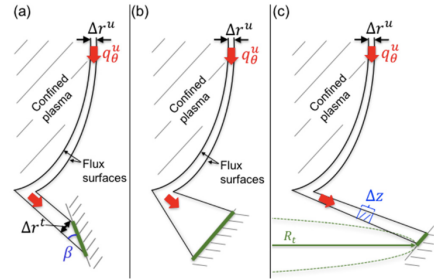
- Geometrical divertor modification can already provide tools for heat flux mitigation



(Theiler *et al.* 2017)

## Geometrical effects on heat flux

- Grazing angle reduce the amount of parallel heat flux perpendicular to the surface  $q_{\perp} = q_{\parallel} \sin \alpha$
- Tilting the divertor plate on the poloidal plane of an angle  $\beta$  already drastically reduce the perpendicular heat flux

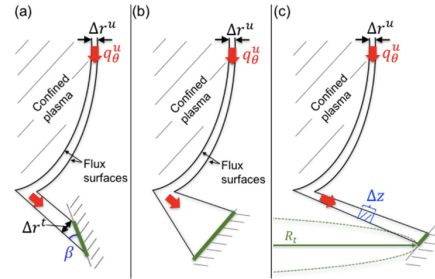


(Theiler *et al.* 2017)

## Geometrical effects on heat flux

- Grazing angle reduce the amount of parallel heat flux perpendicular to the surface  $q_{\perp} = q_{\parallel} \sin \alpha$
- Tilting the divertor plate on the poloidal plane of an angle  $\beta$  already drastically reduce the perpendicular heat flux
- Increase flux-surface separation at the target by increasing the **poloidal flux expansion**

$$f_x = \Delta r_t / \Delta r_u = B_{\theta}^u B_{\phi}^t / B_{\theta}^t B_{\phi}^u$$

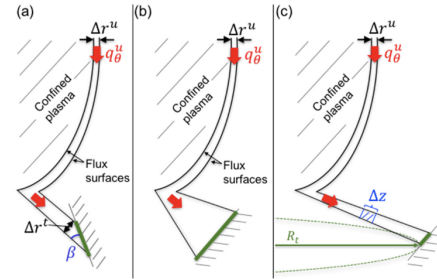


(Theiler *et al.* 2017)

## Geometrical effects on heat flux

- Grazing angle reduce the amount of parallel heat flux perpendicular to the surface  $q_{\perp} = q_{\parallel} \sin \alpha$
- Tilting the divertor plate on the poloidal plane of an angle  $\beta$  already drastically reduce the perpendicular heat flux
- Increase flux-surface separation at the target by increasing the **poloidal flux expansion**

$$f_x = \Delta r_t / \Delta r_u = B_{\theta}^u B_{\phi}^t / B_{\theta}^t B_{\phi}^u$$

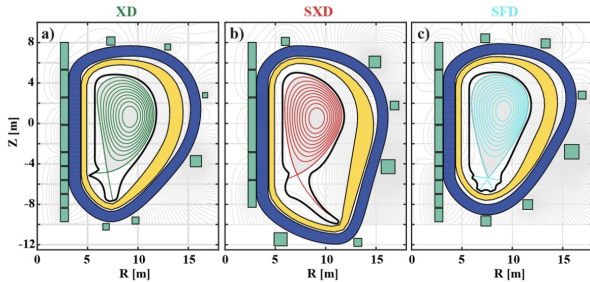


(Theiler *et al.* 2017)

- Increase the target radius. Extension of 2PM to include the variation of the major radius along the divertor leg brings (Kotschenreuther *et al.* 2010; Petrie *et al.* 2013)

$$T_e^t \propto \frac{q_{\parallel}^{10/7} (1 - f_{pow})^2}{n_u^2 L_{\parallel}^{4/7}} \frac{R_u^2}{R_t^2}$$
$$n_e^t \propto \frac{n_u^3 L_{\parallel}^{6/7}}{q_{\parallel}^{8/7} (1 - f_{rad})^2} \frac{R_t^2}{R_u^2}$$

# Alternative divertor configuration

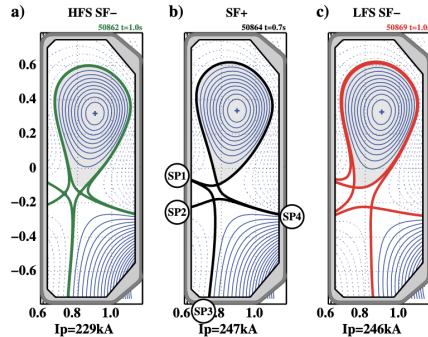


(Reimerdes, Ambrosino, *et al.* 2020)

- Alternative divertor proposed to the standard Lower Single Null adopted for present tokamaks and ITER
- Exploitation of flux flaring at the target (**X-divertor**), of large  $R_t$  effect (**Super-X divertor**)
- Additional solution known as **Snowflake configuration** suggested (Ryutov & Soukhanovskii 2015) with the inclusion of a second X-point

# Alternative divertor configuration

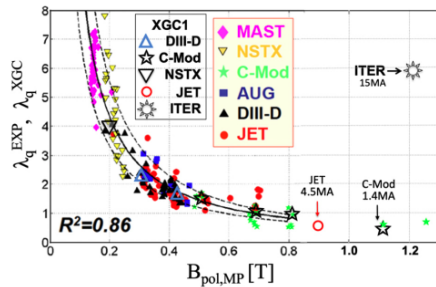
- Zoo of possible SF configuration exists, mainly SF+ and SF- (with second X-point in the private or common flux regione)
- Provide power sharing distribution among the 4 SPs (Maurizio *et al.* 2018), radiation mainly localized within the 2 X-points (Reimerdes, Duval, *et al.* 2017) and modification of SOL transport (Tsui *et al.* 2021)



(Reimerdes, Duval, *et al.* 2017)

## Extrapolation to future devices: the quest for anomalous transport

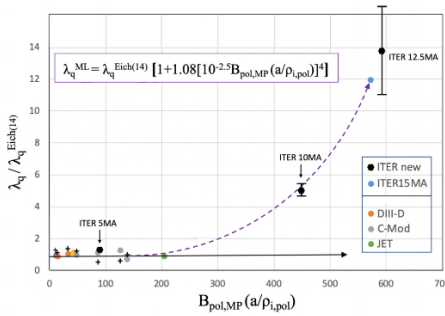
- Present state of the art gyrokinetic code able to mimic the observed scaling (Chang *et al.* 2021)
- Whenever extended to future devices higher  $\lambda_q$  foreseen due to a change of the underlying physical mechanism with TEM in weakly collisional plasma as efficient transported of electron heat and mass



(Chang *et al.* 2021)

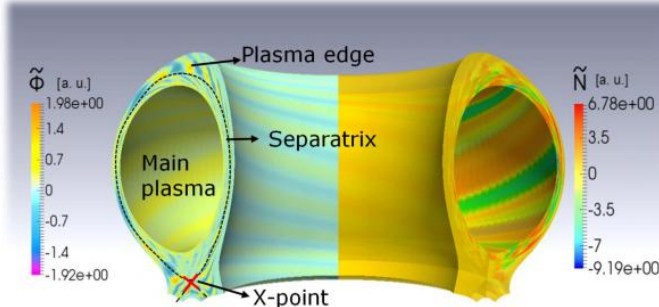
## Extrapolation to future devices: the quest for anomalous transport

- Present state of the art gyrokinetic code able to mimic the observed scaling (Chang *et al.* 2021)
- Whenever extended to future devices higher  $\lambda_q$  foreseen due to a change of the underlying physical mechanism with TEM in weakly collisional plasma as efficient transported of electron heat and mass
- Machine learning approach suggests a scaling compatible with the observed ITPA database as well as giving additional physical insight



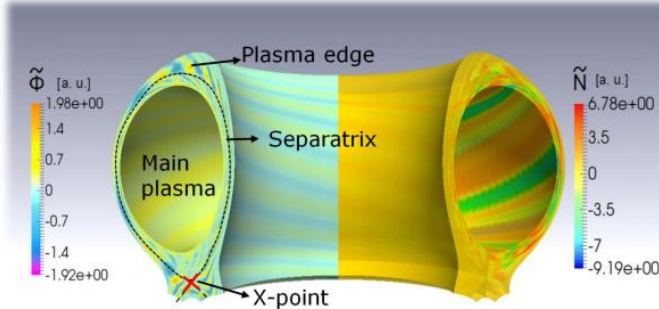
(Chang *et al.* 2021)

## Anomalous transport in the SOL



- In all the approach used so far we concentrate on parallel transport but SOL is a combination between **parallel, perpendicular and sources**.
- The perpendicular transport is strongly **anomalous** with source of free energy coming primarily from separatrix where strong gradient resides (as well as possible damping mechanism as  $\omega_{\mathbf{E} \times \mathbf{B}}$ ). SOL acts as well below the X-point

## Anomalous transport in the SOL



- In all the approach used so far we concentrate on parallel transport but SOL is a combination between **parallel, perpendicular and sources**.
- Various global code currently in development **Tokam3X, GBS, GRILLIX** as example, all including em effects as well as neutrals based on fluid approach. Extension to gyrofluid or gyrokinetic approach in progress

## Conclusions

- We clarify the importance of SOL and Divertor in view of Fusion exploitation
- Divertor and upstream conditions are tightly linked: density and upstream power set the conditions at the target as well as the regime. **True as well the opposite** (e.g. neutral pressure at the target set he  $n_{e,sep}$ )
- A global assessment need an experimental and modeling approach beyond the standard diffusive and 2D SOL approach.
- Remember that PEX is considered as a possible showstopper for fusion exploitation
- Remember this is clearly an incomplete review/lecture where we left apart many topics: PWI, Liquid Divertor, Proper atomic physics occurring at the target ...

## Bibliography i

1. Brunner, D. *et al.* **High-resolution heat flux width measurements at reactor-level magnetic fields and observation of a unified width scaling across confinement regimes in the Alcator C-Mod tokamak.** *Nuclear Fusion* **58**, 094002 (2018).
2. Chang, C. S. *et al.* **Constructing a new predictive scaling formula for ITER's divertor heat-load width informed by a simulation-anchored machine learning.** *Physics of Plasmas* **28**, 022501. ISSN: 1070-664X (2021).
3. Eich, T. *et al.* **Scaling of the tokamak near the scrape-off layer H-mode power width and implications for ITER.** *Nuclear Fusion* **53**, 093031 (2013).
4. Goldston, R. J. *et al.* **A new scaling for divertor detachment.** *Plasma Physics and Controlled Fusion* **59**, 055015 (2017).

5. Huber, A. *et al.* **Improved radiation measurements on JET – First results from an upgraded bolometer system.** *Journal of Nuclear Materials* **363**, 365 (2007).
6. Kallenbach, A. *et al.* **Partial detachment of high power discharges in ASDEX Upgrade.** *Nuclear Fusion* **55** (2015).
7. Kotschenreuther, M. *et al.* **The super X divertor (SXD) and a compact fusion neutron source (CFNS).** *Nuclear Fusion* **50**, 035003 (2010).
8. Maurizio, R. *et al.* **The effect of the secondary x-point on the scrape-off layer transport in the TCV snowflake minus divertor.** *Nuclear Fusion* **59**, 016014 (2018).
9. Petrie, T. W. *et al.* **Effect of changes in separatrix magnetic geometry on divertor behaviour in DIII-D.** *Nuclear Fusion* **53**, 113024 (2013).

10. Pitts, R. et al. **Physics basis for the first ITER tungsten divertor.** *Nuclear Materials and Energy*, 100696 (2019).
11. Pütterich, T. et al. **Determination of the tolerable impurity concentrations in a fusion reactor using a consistent set of cooling factors.** *Nuclear Fusion* **59**, 056013 (2019).
12. Reimerdes, H., Ambrosino, R., et al. **Assessment of alternative divertor configurations as an exhaust solution for DEMO.** *Nuclear Fusion* **60**, 066030 (2020).
13. Reimerdes, H., Duval, B. P., et al. **TCV experiments towards the development of a plasma exhaust solution.** *Nuclear Fusion* **57**, 126007 (2017).
14. Reinke, M. L. **Heat flux mitigation by impurity seeding in high-field tokamaks.** *Nuclear Fusion* **57**, 034004 (2017).

15. Ryutov, D. D. & Soukhanovskii, V. A. **The snowflake divertor.** *Physics of Plasmas (1994-present)* **22**, 110901 (2015).
16. Stangeby, P. C. **Basic physical processes and reduced models for plasma detachment.** *Plasma Physics and Controlled Fusion* **60**, 044022 (2018).
17. Stangeby, P. C. **The Plasma Boundary of Magnetic Fusion Devices.** ISBN: 9780750305594 (Taylor & Francis, 2000).
18. Stangeby, P. **The roles of power loss and momentum-pressure loss in causing particle-detachment in tokamak divertors: I. A heuristic model analysis.** *Plasma Physics and Controlled Fusion* **62**, 025012 (2020).
19. Stangeby, P. **The roles of power loss and momentum-pressure loss in causing particle-detachment in tokamak divertors: II. 2 Point Model analysis that includes recycle power-loss explicitly.** *Plasma Physics and Controlled Fusion* **62**, 025013 (2020).

20. Theiler, C. *et al.* **Results from recent detachment experiments in alternative divertor configurations on TCV.** *Nuclear Fusion* **57**, 072008 (2017).
21. Tsui, C. K. *et al.* **Parallel convection and  $E \times B$  drifts in the TCV snowflake divertor and their effects on target heat-fluxes.** *Nuclear Fusion* **61**, 046004 (2021).
22. Unterberg, B. **Overview of Plasma Edge Physics.** *Fusion Science and Technology* **49**, 215–233 (2017).